The relationship between land surface temperature and local climate zone classification: A case study of the canton Geneva, Switzerland

Maryam Lotfian;
Jens Ingensand;
Sarah Composto
University of Applied Sciences Western Switzerland/GIS-lab/ insit Institute Route de Cheseaux 1
1401 Yverdon-les-Bains, Switzerland {maryam.lotfian , jens.ingensand, sarah.composto}@heig-vd.ch

Monia Molinari;
Maria Antonia Brovelli
Politecnico di Milano, Department of Civil and Environmental Engineering
Piazza Leonardo da Vinci 32
20133 Milan, Italy

{monia.molinari,maria.brovelli}@polimi.com

Abstract

In recent years, urbanization is widely turning into a vital issue due to its impacts on urban climate. It results in many critical problems, such as climate change, air and water pollution, and mainly a well-known phenomenon called Urban Heat Island (UHI), which is defined as the difference of temperature between urban and its surrounding rural areas. The objective of this study is to explore the land surface temperature (LST) differences between urban and rural areas and its relationship with surface characteristics. Accordingly, Landsat8 images were used to obtain a LST map as well as a Local Climate Zone (LCZ) classification map. LCZ is a standard climate-based classification system, which divides the areas according to a surface's physical and thermal properties. Statistical and spatial analysis were used to explore the autocorrelation between LST and LCZ, and the results illustrate that the highly urbanized areas are associated with the highest LST, and areas with dense trees with lowest LST. Interestingly open urban areas with trees around them showed less LST compared to areas with low plants, which can be interpreted in the sense that the effect of trees in cooling strategies is stronger compared to low plants (grass for instance); however, further investigation is required.

Keywords: Urbanization, Urban Heat Island, Local Climate Zone, Image Classification, Land Surface Temperature

1 Introduction

According to the United Nations Department of Economic and Social Affairs projections (United Nations, 2010), the percentage of world population living in urban areas, estimated at 54% in 2014, is likely to rise to 66% by 2050. As a result, cities will steadily become larger and larger and relevant environmental transformations will be required to meet the increasing demand for food, energy, water, and land.

Among the many critical problems resulting from urbanization, Urban Heat Island (UHI) is a well-known issue which refers to the higher temperatures observed in the cities compared to the surrounding rural areas (Oke, 1982, 1976). Many studies have been published over the years that register this urban microclimatic phenomenon in numerous cities around the world regardless of the urban spatial scale (Cardoso et al., 2017; Choi et al., 2014; Pinho and Orgaz, 2000). The primary causes of UHI formation are attributed to urbanization-related triggering factors, which alter the natural surface energy and radiation balances and increase the heat trapping at the surface. For example, the replacement of natural soil and vegetation with sealed building materials (stone, concrete, asphalt, etc.), the 3D urban geometry (built-up ratio, sky view factor, etc.), and the heat generated from anthropogenic activities (combustion, lighting, heating, traffic, etc. (Shahmohamadi et al., 2011)).

If not effectively managed, the UHI phenomenon can have serious implications on the environment and consequently on community's quality of life. Negative impacts suggested by United States Environmental Protection Agency (Hashem, 2008) refers to people's health issues, increase in energy consumption for cooling systems, amplification of air pollution and greenhouse gas emissions problems, and degradation of water quality due to thermal pollution. In light of this, a deeper knowledge about the different climate zones characterizing urban areas is needed to allow urban climate modelling and appropriate mitigation measures adoption.

Over time, several climate-based classification systems have been proposed to study the effect of urbanization and city structure on urban climate (Auer, 1978; Chandler, 1965; Ellefsen, 1991; Oke, 2004). However, the most recent and comprehensive climate-based classification system was developed by Stewart and Oke (Stewart and Oke, 2012) called *Local Climate Zone* (LCZ) classification system. LCZ consists of 17 standard classes which divide both urban and rural areas to "built types" and "Land-cover types" mainly based on the characteristics of surface structure (buildings and trees height and density), and surface cover (impervious and pervious) (Stewart and Oke, 2012). The surface properties such as vegetation fraction, building/tree height, and anthropogenic

heat flux, which directly affect the screen height temperature, make the zones distinguishable from each other (Stewart and Oke, 2006). Detailed guidance on how to perform a LCZ classification map is given in a global project called WUDAPT (World Urban Database and Access Portal Tool) (Bechtel et al., 2015).

Several studies have investigated the effects of land surface characteristics on land surface temperature (LST). A research project exploring the relationship between LST and land surface properties (vegetation and built up) in Nairobi (Mwangi et al., 2018), illustrated that LST is negatively correlated with Normalized Density Vegetation Index (NDVI), and positively correlated with Built-Up Density Index (BDI). Another study in Budapest (Szegediensis, 2016), investigated the effects of greenery on LST, and results showed a significant difference of LST (40 °C on 02 August, 2014) between compact built areas and areas with dense trees.

Therefore, this paper aims at investigating the relationship between LCZ classification and LST in the canton of Geneva in Switzerland. To explore the latter association, some exploratory spatial data analysis and remote sensing approaches have been applied and will be discussed in the following sections.

2 Previous work

TherSol was a project done in Geneva, Switzerland, from 2014 to 2016 aiming at exploring the influence of ground surfaces on urban climate (Ingensand et al., 2016). More specifically, the main goals of this project were to identify significant types of urban soil and to highlight the impact of these identified soil types on urban microclimate. In order to accomplish these goals, the area around Plainpalais in the city of Geneva was selected, which is a flat open area with three very different soil types such as red brick aggregates, asphalt, and lawn (Figure 1). Based on the various soil types, 15 zones were determined in this area, and meteorological observations including temperature at different heights above the ground (from 20 to 250 centimeters), air humidity, solar irradiation, wind speed, and wind direction were collected within the zones. The data were acquired using a backpack equipped with thermometers during four days in June, July, and August in 2015. The variation of the measures within the 15 zones were analyzed, and the results highlighted that the permeable surfaces in urbanized areas significantly decrease the risk of UHI phenomenon. To expand this experiment for the entire canton of Geneva, all the surface types and measures are required, while obtaining such observations for a large region, requires a considerable amount of time and money. Therefore, this study presents a LCZ classification approach to address the effects of surface covers on urban climate and as a result UHI phenomenon.

Figure 1: The area of Plainpalais in Geneva, lawn (green dot), red brick aggregates (red dot), and asphalt (blue dot)

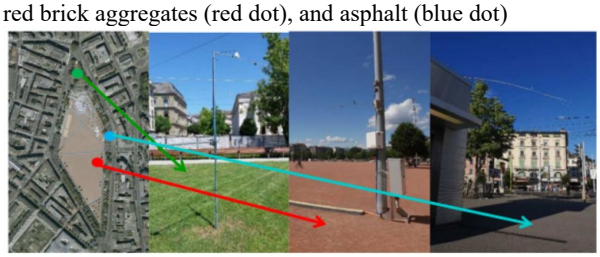

3 Methods

The methodology consists of three parts, first the creation of a LCZ classification map, second the computation of the LST, and finally the exploration and association between the two using spatial and statistical analysis.

3.1 LCZ classification

The methodology of producing a LCZ classification map is based on our previous work (Lotfian, 2016). A pixel-based supervised classification approach with Random Forest algorithm has been used. Figure 2 illustrates the flowchart of the specific iterative methodology, which needs to be followed to obtain the LCZ classification map. The first operations in this process are the manipulation of the raw data. They include the digitization of the training data for the supervised classification and the pre-processing of the satellite images. In this case study, the training areas are obtained according to the characteristics of LCZ classification system, and 8 of the 17 possible classes were found and considered as the main ones for our region of interest (Table 1). The second step regards the pre-processing operations of the satellite images. In fact, Landsat8 images are clipped according to the region of interest, and all the bands are resampled into 100m spatial resolution grid and merged together to create a layer stack. These operations have been mainly performed in QGIS (www.qgis.org). Finally, the random forest algorithm is applied. In this study, Random Forest has been implemented using both the open source programming software R and in the open source program SAGA GIS, and the results were compared between the two approaches. As results, R fits better the comparison and thus it is used in this methodology. In fact, R runs the classification faster compared to SAGA, with less steps of operation (such as Geo-referencing and merging the training areas) and the "out-of-bag (OOB)" error and confusion matrix are obtained at the end of the procedure. As the output of the random forest classification from R tends to be noisy, a post-classification filter is needed. In this work, a majority filter with the neighborhood of 1px is applied using QGIS, as it change the pixel values based on the value of their contiguous pixels. It is possible to test the majority filtering using different neighborhoods, depending on the desired output.

Figure 2: Flowchart describing the methodological approach used to generate the LCZ classification map

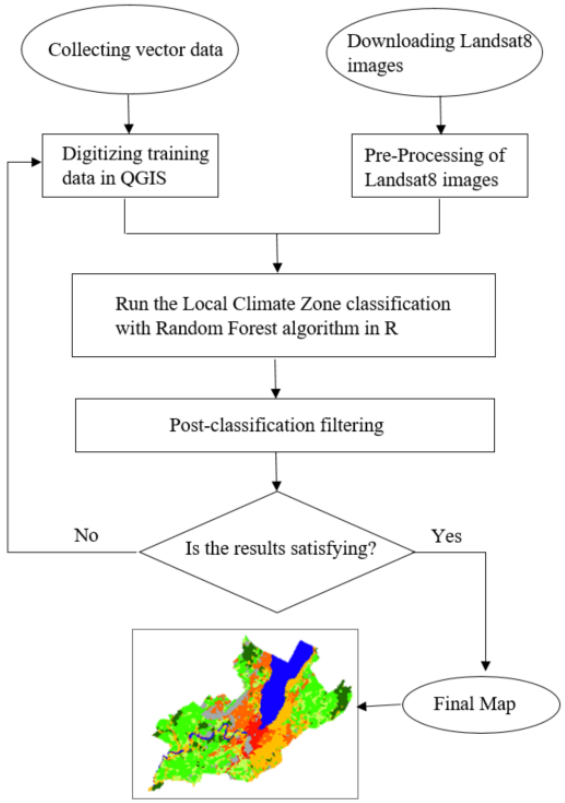

Table 1: Local Climate Zone (LCZ) classes retained for canton of Geneva (Stewart and Oke, 2012). Class ID corresponds to the assigned IDs for our classification not the LCZ standard class numbers

ID	Class name	Description
1	Compact mid-rise	Dense mix of midrise buildings (3–9 stories). Few or no trees. Land cover mostly paved. Stone, brick, tile, and concrete construction material.
2	Open mid-rise	Open arrangement of midrise buildings (3–9 stories). Abundance of pervious land cover (low plants, scattered trees). Concrete, steel, stone, and glass construction materials
3	Open low-rise	Open arrangement of low-rise buildings (1–3 stories). Abundance of pervious land cover (low plants, scattered trees). Wood, brick, stone, tile, and concrete construction materials
4	Industrial (large low-rise)	Open arrangement of large low-rise buildings (1–3 stories). Few or no trees. Land cover mostly paved. Steel, concrete, metal, and stone construction materials.
5	Sparsely built	Sparse arrangement of small or medium-sized buildings in a natural setting.
6	low plant	Featureless landscape of glass or herbaceous plants/crops. Few or no trees. Zone function is natural grassland, agriculture, or urban park
7	Dense trees	Heavily wooded landscape of deciduous and/or evergreen trees. Land cover mostly pervious (low plants).
8	Water	Large, open water bodies such as seas and lakes, or small bodies such as rivers, reservoirs and lagoons.

3.2 LST map

The LST is obtained using a procedure defined by Avdan and Jovanovska (Avdan and Jovanovska, 2016). The authors have used band10 (thermal), band5 (NIR), and band4 (red) of Landsat8 images to obtain the LST in degrees of Celsius. We have followed their methodology by developing an R script, which obtains the three mentioned bands as the input data and that produces the LST map in the Geo-Tiff format. Figure 3 illustrates the steps to be followed to retrieve the LST from any Landsat8 image.

3.3 Statistical analysis

To explore the overall variation of LST within the LCZ classes, box plots and 95% confidence intervals of LST values in each class were generated in R.

Moreover, to investigate the spatial autocorrelation between the two variables, global spatial autocorrelation Moran's I, and Local Indicators of Spatial Association (LISA) (Anselin, 1995) implemented in GeoDa software (Anselin and Mccann, 2009) were used.

Moran's I statistics evaluates the existence of global spatial clusters in the dataset, and it uses one measure to summarize the whole study area, which can be computed as illustrated in Equation 1.

Equation 1: Moran's I statistic

$$I = \frac{N \Sigma i \Sigma j Wij(Xi - \overline{X})(Xj - \overline{X})}{(\Sigma i \Sigma j Wij)\Sigma i(Xi - \overline{X})^2}$$

Where

- N is the number of observation units
- Wij is the spatial weight
- Xi is the value at location i
- Xj is the value at location j
- $\overline{X}$ is the mean of the variable

LISA statistics on the other hand locally identifies the regions where variables are strongly positively or negatively correlated. As a result of LISA analysis, a Moran's I scatter plot, a cluster map, and a significance map were obtained. Moran's I coefficient ranges from -1 to 1 indicating a global spatial autocorrelation, positive values illustrate spatial similarity, negative values show dispersion or spatial dissimilarity, and zero means no spatial autocorrelation. The cluster map generates four clusters: High-high, low-high, low-low, and high-low, where high-high indicates variables with high values surrounded by high values, low-high indicates variables with low values surrounded by low values, and likewise for low-low and high-low. Finally, the significance map shows at which statistical levels there are significant correlations.

To compute LISA, a weighting scheme of four nearest neighbors were applied, and for the statistical significance testing a sample of 999 permutations were used.

Figure 3: Calculation of Land Surface Temperature from band10, band5, and band4 of Landsat8 images

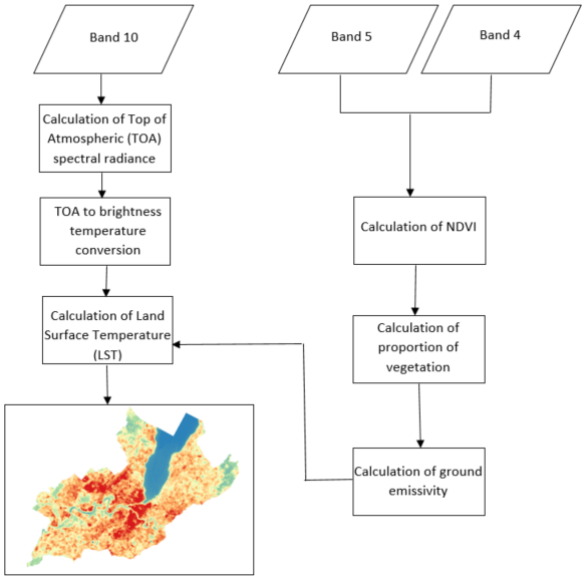

4 Results

4.1 LCZ classification

Figure 4 illustrates the LCZ classification map obtained from Landsat8 image of 26 June 2018. The OOB error obtained from random forest was 0.07, which means the overall accuracy of the classification is 93%. Due to spatial autocorrelation between the training and testing datasets, the overall accuracy of spatial data in random forest algorithm tends to be overestimated. It is usually suggested to use a separate testing dataset to obtain the overall accuracy; however, for the objective of this study the accuracy assessment obtained from random forest was sufficient; therefore, a separate testing dataset was not used.

4.2 Land Surface Temperature

Figure 5 shows the LST map generated from the same Landsat8 image as LCZ classification. The map illustrates the spatial distribution of surface temperature in the canton of Geneva. It is shown that the hottest areas are mainly located in the center and north-west of the canton, which are the highly built urban zones with impervious surfaces materials, and as we go further from the center, the LST decreases. On the other hand, the water bodies and areas with dense trees are associated with lowest surface temperature.

4.3 LCZ and LST

The box plots generated for LST values versus different LCZ classes are shown in Figure 6. The results illustrate clear variation of LST with respect to LCZs. LCZ1 (compact mid-rise) and LCZ4 (large low-rise), followed by LCZ2 (open mid-rise), were the first and second hottest zones respectively. While as illustrated in the LST map, LCZ8 (water) and LCZ7 (dense trees) had the lowest surface temperature. The two non-urban classes, sparsely built, and low plants did not show a considerable difference (slightly higher) compared to the urban class open low-rise. In addition to the box plots, the 95% confidence intervals of mean LST is presented in Figure 7, which illustrates a more perceptible variation of LST within the LCZs; a difference of 18°C between LCZ1 and LCZ7 were observed.

In addition, the results from LISA cluster map (Figure 8) illustrated that 20229 pixels showed no spatial autocorrelation between LST and LCZ, whereas 3736 pixels were clustered as low-high (low temperature surrounded by high LCZ values according to the numbers presented in Table 1), and 3504 pixels as high-low. There were only few pixels clustered as high-high and low-low with 2 and 247 pixels respectively. Furthermore, the significance map (Figure 9) showed 4331 cells significantly auto-correlated at p-value 0.001 and 3158 cells at p-value 0.01. The overall Moran's I coefficient was -0.62, which indicates a strong negative spatial association between LST and LCZs.

Figure 4: Local Climate Zone Classification map with spatial resolution of 100m. Low-rise and mid-rise represents the buildings' heights, 3-10 meters and 10-25 meters respectively

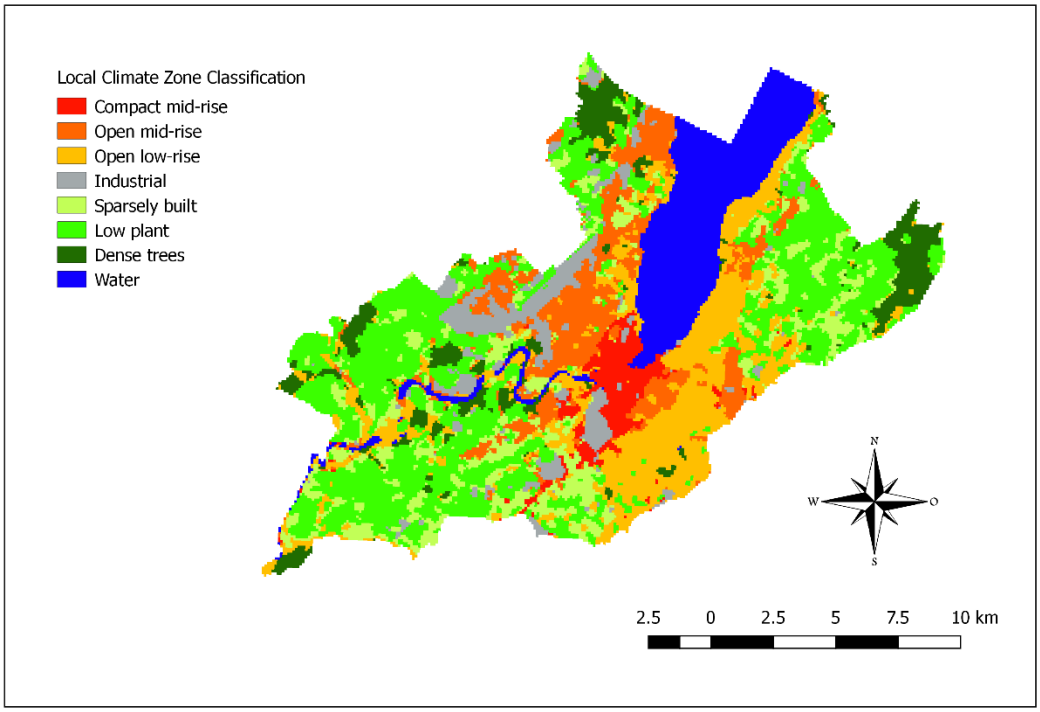

Figure 5: Land surface temperature map of Geneva canton, temperature is in degrees of Celsius

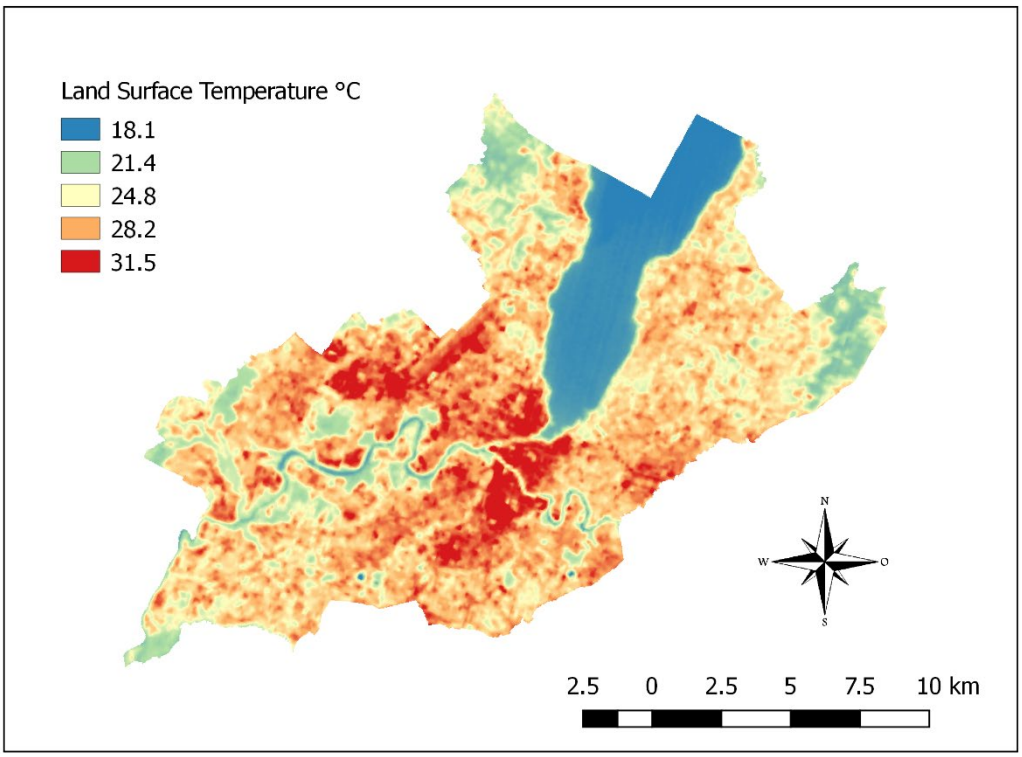

Figure 6: Box plots of LST for each LCZ class. The numbers in x-axis corresponds to the LCZ classes

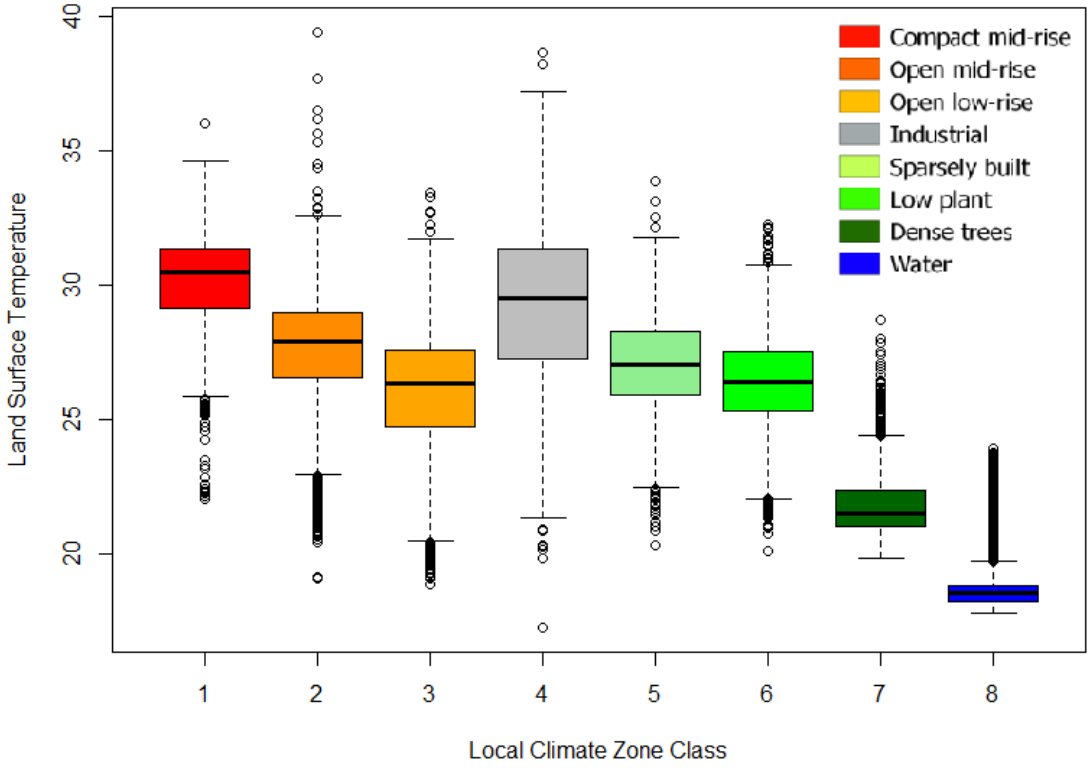

Figure 7: 95% confidence intervals of mean land surface temperature within each local climate zone class

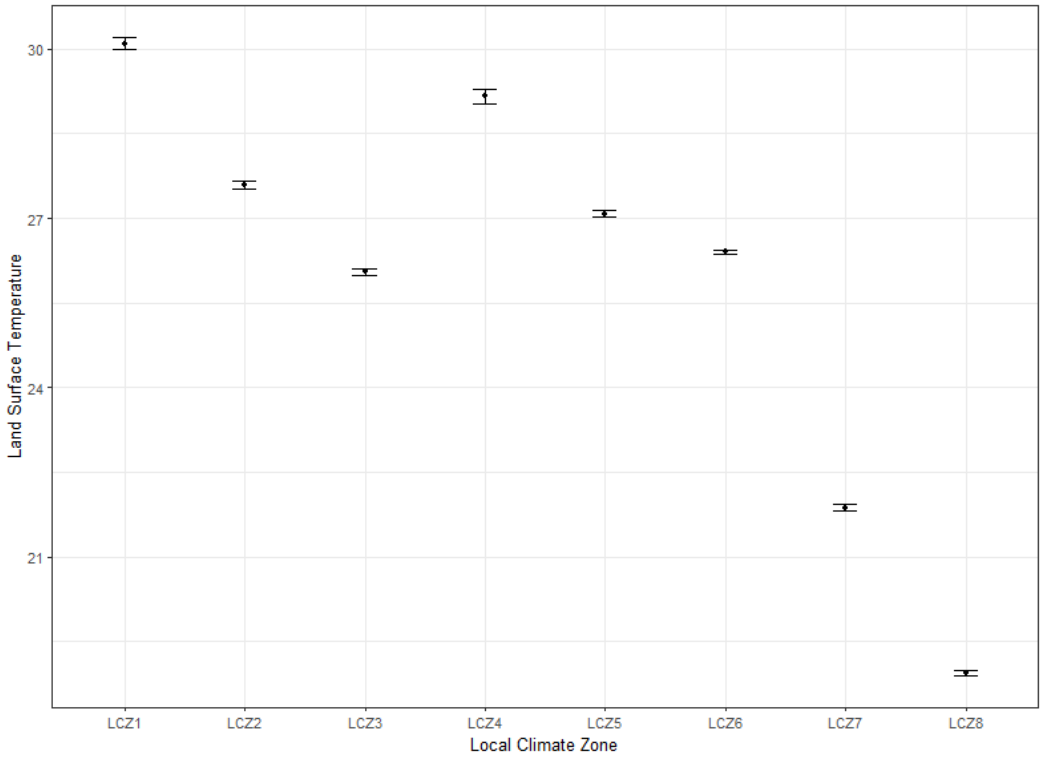

Figure 8: LISA cluster map. The map represents where there are spatial positive or negative autocorrelation between LST and LCZs classes, and clusters the values accordingly. First variable is LST and second LCZ. Background map: Landsat8 image

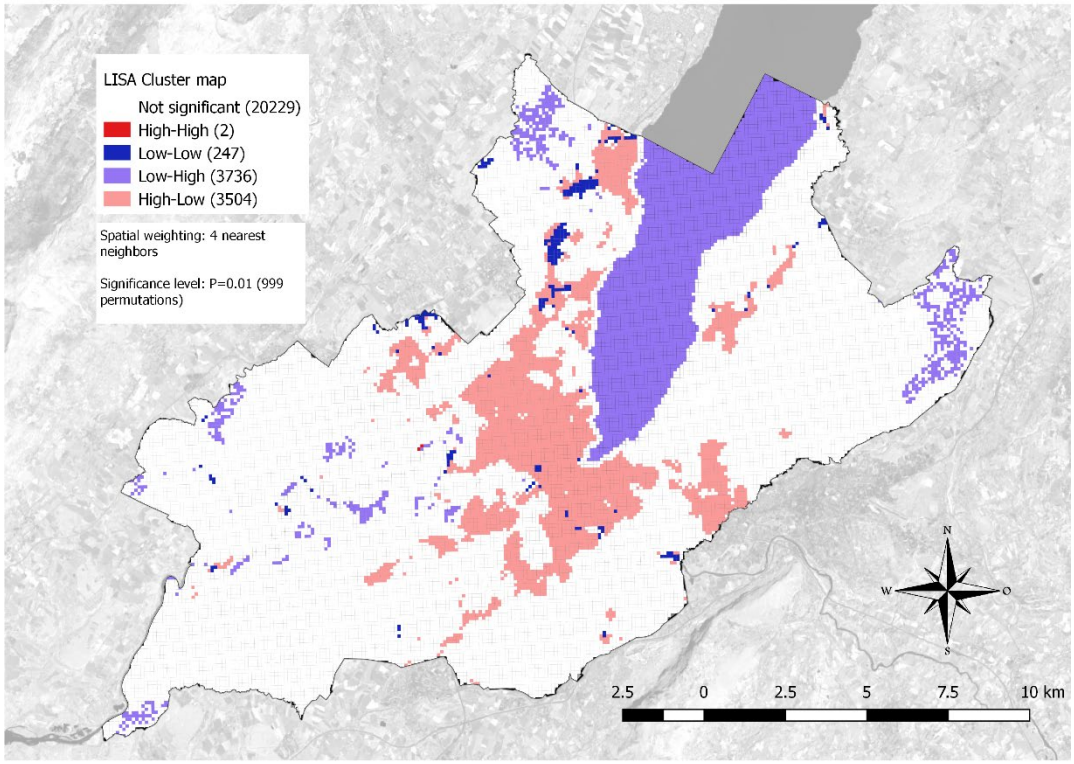

Figure 9: LISA significance map. The map illustrates where LISA clusters are statistically significant and at which significance level. Background map: Landsat8 image

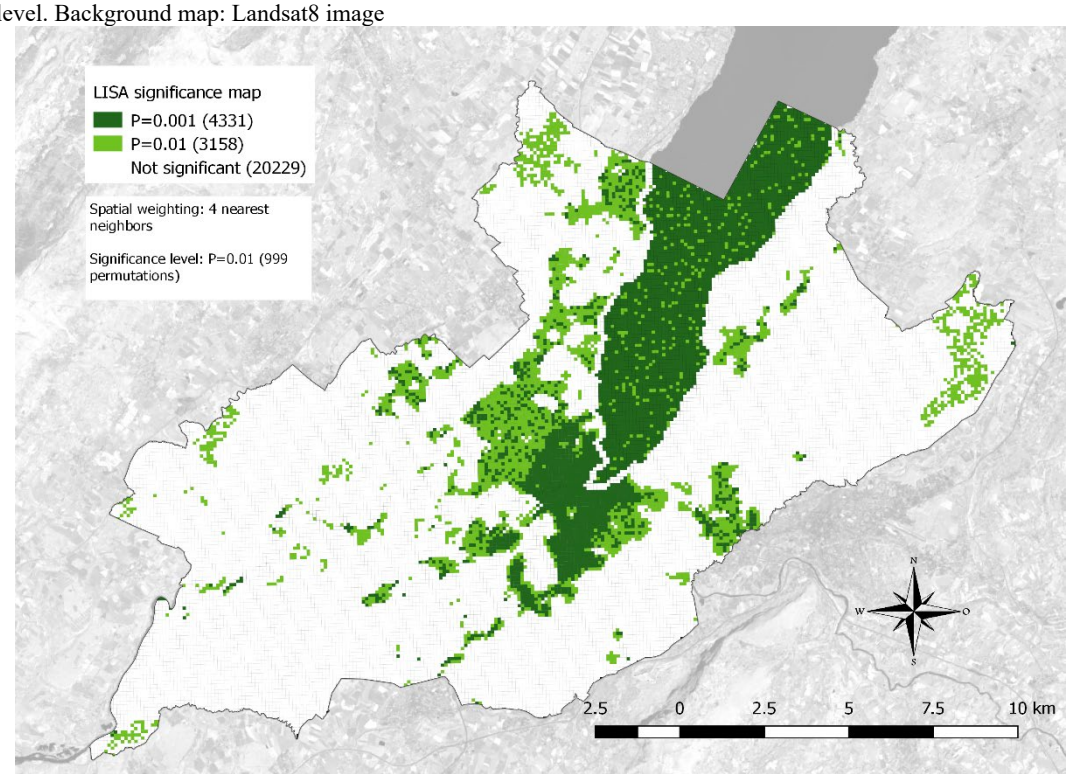

5 Discussion

The spatial distribution of UHI can be determined thorough the LCZ classification, as this scheme is based on surface thermal characteristics. Analyzing the box plots, it is clearly observable that the behavior of urban and non-urban classes with respect to temperature are opposite to each other. For dense trees and water the high temperature values are outliers, on the contrary for the urbanized zones the outliers are associated with low temperature values. The 95% confidence intervals for mean LST within each LCZ classes illustrated that there are statistically significant differences. The LISA cluster map highlighted a clear association between LST and LCZ variables; the compact mid-rise and open mid-rise areas fall mainly within High-Low clusters whereas dense trees and water bodies in Low-High clusters. The contribution of extreme classes such as compact mid-rise, dense trees, and water on LST values were significantly observable compared to the other ones. Surprisingly, low plants and sparsely built classes, which are located in the surrounding rural areas showed higher values of LST compared to the open low-rise, which is an urban type class. This can be due to the fact that LCZ open low-rise is mainly located near the lake-side and it consists of low buildings (such as villas) with trees around them, and it appears (from dense trees class) that the effect of trees on reducing the temperature is stronger compared to low plants. The results highlights the hot spots and their associated surface cover types (specially in urban areas), which can be a very useful input for urban planners and urban architects for decision makings with respect to heat mitigation strategies such as choices in surface materials, planting trees, increasing surface albedo, etc.

6 Conclusions and prespectives

Due to an increase in urbanization and as a result changes in land cover, which create the so-called urban heat island (UHI) phenomenon, this study focuses on the effect of surface characteristics on land surface temperature in the canton of Geneva. Hence, from Landsat8 images, LCZ classification map and LST map were obtained, and subsequently LISA statistics were used to explore the local spatial auto-correlation between the two obtained variables. Results illustrated that urbanized areas with high dense buildings have higher values of land surface temperature compared to the areas with high levels of vegetation especially dense trees. Nonetheless, to enhance the results and to avoid biased outcome it is better to check the analysis over different times of the year mostly because of the varieties in degrees of vegetation over different seasons. This approach is going to be applied in different cities and to compare the results afterwards to explore the various factors causing UHI as well as understanding how this can help urban planners and urban policy makers to take actions towards sustainable urban development.

References

Anselin, L., 1995. Local Indicators of Spatial Association-LISA. Geogr. Anal. 27.

Anselin, L., Mccann, M., 2009. OpenGeoDa , Open Source Software for the Exploration and Visualization of Geospatial Data 550–551.

Auer, A.H., 1978. Correlation of Land Use and Cover with Meteorological Anomalies. J. Appl. Meteorol.

Avdan, U., Jovanovska, G., 2016. Algorithm for Automated Mapping of Land Surface Temperature Using LANDSAT 8 Satellite Data 2016.

Bechtel, B., Alexander, P., Böhner, J., Ching, J., Conrad, O., Feddema, J., Mills, G., See, L., Stewart, I., 2015. Mapping Local Climate Zones for a Worldwide Database of the Form and Function of Cities. ISPRS Int. J. Geo-Information 4, 199–219.

Cardoso, R., Dorigon, L., Teixeira, D., Amorim, M., 2017. Assessment of Urban Heat Islands in Small- and Mid-Sized Cities in Brazil. Climate 5, 14.

Chandler, T., 1965. The Climate Of London. London: Hutchinson.

Choi, Y.-Y., Suh, M.-S., Park, K.-H., 2014. Assessment of Surface Urban Heat Islands over Three Megacities in East Asia Using Land Surface Temperature Data Retrieved from COMS. Remote Sens. 6, 5852–5867.

Ellefsen, R., 1991. Mapping and measuring buildings in the canopy boundary layer in ten U.S. cities. Energy Build. 16, 1025–1049.

Hashem, A., 2008. Reducing Urban Heat Islands: Compendium of Strategies Urban Heat Island Basics 1–22.

Ingensand, J., Bullinger, G., Composto, S., Spahni, B., Froidevaux, M., Nappez, M., Varesano, D., 2016. The influence of ground surfaces on urban climate 2015–2016.

Lotfian, M., 2016. Urban Climate Modeling, Case study of Milan city. Master Thesis, School of Civil Environmental and Land Management Engineering. Politecnico di Milano.

Mwangi, P.W., Karanja, F.N., Kamau, P.K., 2018. Analysis of the Relationship between Land Surface Temperature and Vegetation and Built-Up Indices in Upper-Hill , Nairobi 1–16.

Oke, T.R., 1976. The distinction between canopy and boundary layer urban heat islands. Atmosphere (Basel). 14, 268–277.

Oke, T.R., 1982. The energetic basis of the urban heat island. Q. J. R. Meteorol. Soc. 108, 1–24.

Oke, T.R., 2004. Initial guidance to obtain representative meteorological observations at urban sites. World Meteorol. Organ. 51.

Pinho, O.S., Orgaz, M.D., 2000. The urban heat island in a small city in coastal Portugal. Int. J. Biometeorol. 44, 198–203.

Shahmohamadi, P., Che-Ani, A.I., Maulud, K.N.A., Tawil, N.M., Abdullah, N.A.G., 2011. The Impact of Anthropogenic Heat on Formation of Urban Heat Island

and Energy Consumption Balance. Urban Stud. Res. 2011, 1–9.

Stewart, I., Oke, T., 2006. Thermal differentation of local climate zones using temperature observations from urban and rural areas. Univ. Br. Columbia.

Stewart, I.D., Oke, T.R., 2012. Local climate zones for urban temperature studies. Bull. Am. Meteorol. Soc. 93, 1879–1900.

Szegediensis, U., 2016. Analysis of land surface temperature and ndvi distribution for budapest using landsat 7 etm+ data g molnár 49–61.

United Nations, 2010. World Urbanization Prospects: The 2009 Revision. Popul. Dev. Rev. ESA/P/WP/2, 56.